IEEE Access
Multidisciplinary | Rapid Review | Open Access Journal

Received August 31, 2021, accepted September 28, 2021, date of publication October 4, 2021, date of current version October 12, 2021.

Digital Object Identifier 10.1109/ACCESS.2021.3117395

Analysis of Electromagnetic Pulse Effects Under High-Power Microwave Sources

SUN-HONG MIN[1], HOECHUN JUNG[2], OHJOON KWON[3], MATLABJON SATTOROV[4,5,6], SEONTAE KIM[4,5,6,7], SEUNG-HYUK PARK[8], DONGPYO HONG[4,5,6], SEONMYEONG KIM[4,5,6], CHAWON PARK[1], BONG HWAN HONG[1], ILSUNG CHO[1], SUKHWAL MA[1], MINHO KIM[1], YOUNG JOON YOO[5], SANG YOON PARK[5], AND GUN-SIK PARK[4,5,6], (Senior Member, IEEE)

[1]Korea Institute of Radiological and Medical Sciences (KIRAMS), Seoul 01812, South Korea
[2]Rare Isotope Science Project, Institute for Basic Science, Daejeon 34047, South Korea
[3]Institute for Basic Science, Center for Axion and Precision Physics Research, Daejeon 34141, South Korea
[4]Center for THz-Driven Biomedical Systems, Department of Physics and Astronomy, College of Natural Sciences, Seoul National University, Seoul 08826, South Korea
[5]Center for Applied Electromagnetic Research, Advanced Institutes of Convergence Technology, Suwon, Gyeonggi-do 16229, South Korea
[6]Department of Research and Development, Seoul-Teracom Inc., Suwon 16229, South Korea
[7]Young IN ACE, Dongan-gu, Anyang-si, Gyeonggi-do 14042, South Korea
[8]Hanwha Corporation, Gumi 730-030, South Korea

Corresponding author: Gun-Sik Park (gunsik@snu.ac.kr)

This work was supported in part by the National Research Foundation of Korea (NRF) funded by the Government of Korea [Ministry of Science and ICT (MSIT)] under Grant NRF-2021M2E8A1038938, Grant NRF-2021R1F1A1048374, and Grant NRF-2016R1A3B1908336; and in part by Korea Institute of Radiological and Medical Sciences (KIRAMS) funded by MSIT, Republic of Korea, under Grant 50051-2021, Grant 50623-2021, and Grant 50532-2021.

ABSTRACT High-power microwave sources applied to a directed-energy weapon can lead to permanent damage by radiating concentrated energy in a specific direction to disturb or overload electronic equipment. The effect analysis on the target, such as electronics exposed to electromagnetic pulse, should be considered as an important factor in determining the performance of high-power microwave sources and conducting experimental evaluations. In this study, a magnetically insulated transmission line oscillator, one of the representative high-power microwave sources based on vacuum electronics device, was constructed and experimental analysis with respect to electromagnetic pulse effects was performed. The specification of the magnetically insulated transmission line oscillator used in this study corresponded to 3 GW of high-power electromagnetic wave pulses operating at L-band. The power efficiency was approximately 10 – 15%. For effective targeting, a Vlasov antenna that converts TM_{01} mode to TE_{11} mode was designed and fabricated. The radiation pattern was confirmed via fluorescent lamps, and to confirm the effect of the directed-energy weapon on the target, an effect analysis was performed using a portable electronic device as a sample. Furthermore, the electric field was measured with a D-dot probe and quantified and compared. This study presents a future blueprint of the value of the directed-energy weapon by predicting the radiant output power of the weapon in the far-field region after it is mounted on a movable ground vehicle or unmanned aerial vehicle.

INDEX TERMS High power microwave (HPM), directed-energy weapon (DEW), electromagnetic pulse (EMP), magnetically insulated transmission line oscillator (MILO).

I. INTRODUCTION

The development of pulse power machines (PPMs) led to the emergence of high-power microwave (HPM) sources that create a relativistic beam. The process of generating an electric field via HPM sources that generate a relativistic electron beam requires the development of a more intensive and high-voltage pulsed power generator. HPM generation is of significant interest in a laboratory because a PPM, which is stored as a capacitor and generates a high voltage, occupies a large volume and has a large mass. Hence, PPM, which stores high voltage as a capacitor, is mainly used as a HPM source because it requires a generator with a constant impedance of several tens of hundreds to thousands

The associate editor coordinating the review of this manuscript and approving it for publication was Debdeep Sarkar.

of kV for 100 ns. The energy circuit stored in the capacitor is highly suitable for pulses of approximately 100 ns with high voltage and high output. High-power microwave technology is one of the most recent technologies, and new innovations and applications in this technology and can be applied to new applications [1]–[3]. A quantum leap with respect to the level of microwave power can be used to guide physics in new directions with conventional microwave equipment or new interaction mechanisms in the microscopic world. Conventional microwave electronics can reverse the current trend toward miniaturization of solid-state devices. They inherently exhibit limited output capacity [4]–[6]. HPM generation can lead to generation of enormous power, and thus it can be considered as a significant factor in the future as an energy source for modern relativistic electron beam technology. These high-power microwaves are applied to military weapons, such electromagnetic pulses (EMPs), based on directed-energy weapons (DEWs). Over the past two decades, extensive research has been conducted on EMP weapons that directly transmit energy as opposed to other transmission methods [7]–[12].

HPM devices have been developed since 1960s, starting with gyrotron, free electron laser (FEL), vircator, klystron, magnetron, and relativistic magnetron (RM), which can handle electrons in a relativistic realm by accelerating excessively high-voltage electrons. HPM based high-power electromagnetic wave pulse generators, such as magnetically insulated transmission line oscillator (MILO), backward wave oscillator (BWO), and traveling wave tube (TWT) have been proposed and developed. Furthermore, the impulse source that enables RF radiation of high-power electromagnetic waves in a wider area through an antenna has been continuously developed. Moreover, the pulsed electron beam (e-beam) accelerator required to generate the HPM presents a major concern, and compression of the pulses within the PPM can result in a relativistic electron beam. Hence, this principle can be applied to EMPs termed as an electronic bomb [13]–[26].

Most recently, drone strikes have dramatically changed the face of warfare. This presents a new opportunity, especially for terrorists, as it can transform small commercial drones into weapons of terrorism. Without any armament, only the kinetic energy of the drone is sufficient to attack a person or collide with an aircraft near an airport. Therefore, prevention of drone attacks and terrorism is emerging as a new security challenge. Hence, a wide array of ideas, including lasers and anti-aircraft guns to attack drones, electromagnetic jammers and even nets for capturing drones, and eagles have emerged. Specifically, the use of electromagnetic waves in a drone shooting system is not a new idea. Some systems, such as guns, can be carried and fired by an individual. However, considering the power and range, a stationary system that can also move in a vehicle can block drones more effectively. The EMP attack system is the safest method for preventing simultaneous attacks from multiple drones, especially when protecting facilities that are sensitive to the use of firearms or facilities with civilians nearby [27]–[37].

In this study, the EMP effect on electronic devices was analyzed by designing and manufacturing a narrowband oscillator termed as MILO. Hence, based on theory, design, manufacturing, and testing of pulse power devices, a Marx generator with an electron beam acceleration energy of up to 1 MeV, which can generate GW-class high-output pulse power from a relatively low voltage (of several tens of kV), was designed and manufactured. Furthermore, a pulse forming device, Blumlein pulse forming line device, was designed and manufactured. High output pulse power of GW-level was generated from this system [38]. The power level was confirmed with diagnostic devices such as voltage probe and magnetic-variable probe. Based on the design and fabrication of MILO, a device was designed and manufactured to generate high-power microwaves from the electron beam generated by the pulse power device via theoretical calculations and simulations. Additionally, to test this device, a microwave diagnostic device was designed and manufactured. To ensure accurate targeting, TM_{01} mode, which is the basic mode that occurs in the MILO circuit, was converted to TE_{11} mode. Hence, a Vlasov antenna with optimal gain was designed, manufactured, and demonstrated. Additionally, the performance of the antenna was evaluated. A maximum output of approximately 3 GW of L-band (1.15 GHz) was obtained for 50 ns with an output efficiency in the approximate range of 10–15%. Finally, by conducting analysis of radiation patterns and effects on electronic devices. guidelines and blueprints are presented for application to EMPs in future studies.

II. MILO SYSTEM

A. MILO EQUIPPED WITH A PULSED E-BEAM ACCELERATOR

As mentioned earlier, we adopted the MILO system as a source of HMP for EMP application research. MILO is considered as a vacuum element that can generate the highest level of power among the existing sources of HPM. Furthermore, other organizations worldwide are also developing it as an EMP device. The performance specifications of the pulsed electron beam accelerator, applied in this study, were verified in our previous study. Additionally, the reproducibility of design, circuit fabrication, and performance experimental studies based on theoretical research on MILO was confirmed in prior research. In this study, we focus on mode competition in MILO, which is considered as an HPM generator. It has been experimentally and theoretically proven that this mode competition can lead to unstable operation, an important issue in HPM generators. Specifically, mode competition was observed via the waveguide at the output stage and microwave B-dot sensor installed in each resonator. In the observed mode competition phenomenon, in contrast to normal mode competition, the fast-growing axial mode close to the desired π-mode grows initially, but eventually

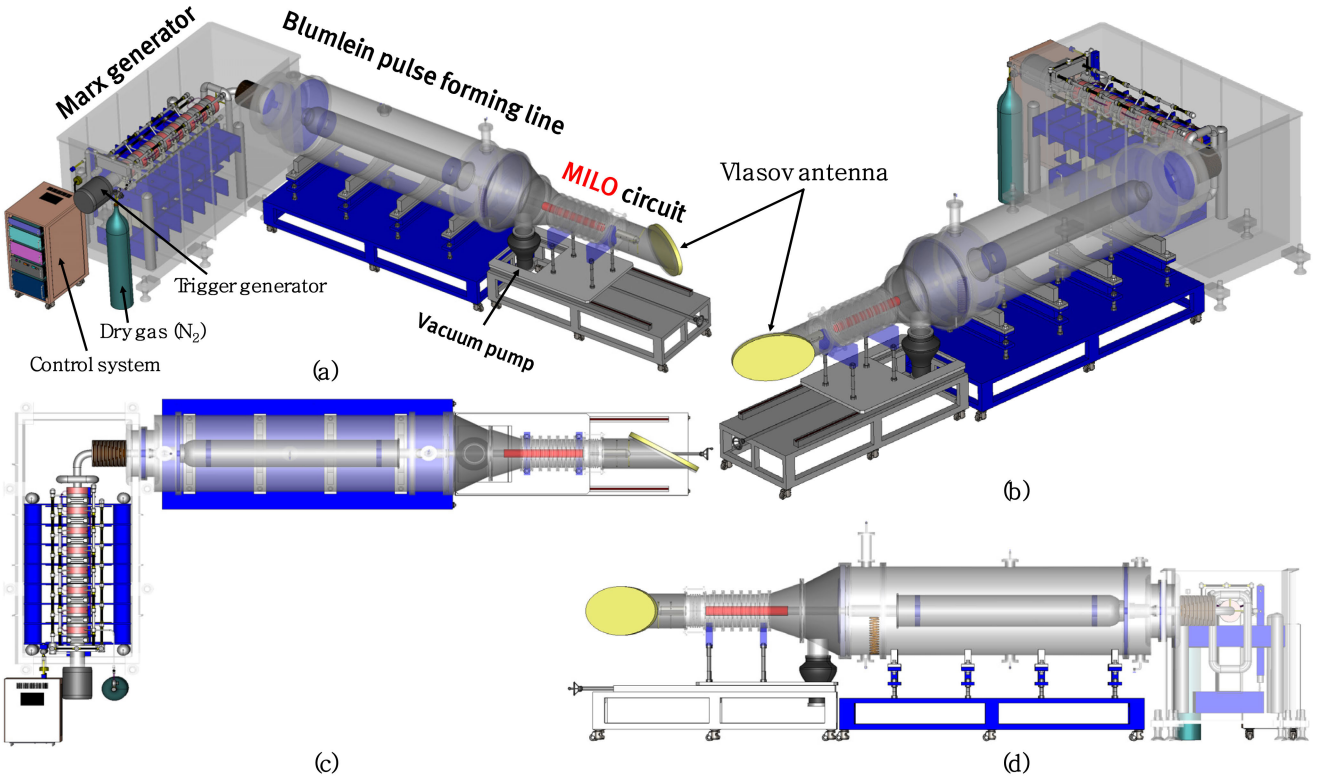

FIGURE 1. MILO system as a representative HPM source for application to an EMP generator; (a) Outline of 3D modeling design applicable to EMP, (b) 3D aerial view of MILO system with Vlasov antenna center view, (c) top view of the MILO system, and (d) side view of the MILO system.

shifts to a slow-growing stable mode. We determined that the kinetics of this mode competition is highly dependent on the temporal change of the magnetically insulated electron beam drift velocity. This is related to the dependence on the pulse shortening phenomenon according to the output power. The influence of the anode plasma generated between the cathode and anode of the diode was confirmed in a previous experimental study [21].

To verify the performance of MILO, a pulse power device capable of accelerating an electron beam to a maximum of 1 MeV with a maximum acceleration voltage of 800 kV and variable impedance control based on the property conservation law were used. In the case of a diode impedance characteristic of approximately 14 Ω, MILO can generate up to 45 GW of electron beam. By using this electron beam to generate electromagnetic waves with a power efficiency of 10–15%, it was possible to create an RF output power of 3 GW. Additionally, based on previous research results, the rise time of RF output is formed in several tens of ns. Therefore, based on the 100–150-ns pulsed electron beam accelerator used in this experimental study, an RF output power of 20–50 ns can be realized [38].

Fig. 1 shows the three-dimensional model of the MILO system. Fig. for the theoretical study, design data, and production performed in advance. Based on the 3D modeling results shown in Fig. 1, the reproducibility of the MILO system is sufficiently secured through more than 1000 shots. This was conducted in a prior study to build a reliable database for performance verification. Fig. 1-(a) shows a Marx generator filled with insulated oil and trigger generator consisting of R-L-C circuits for high-voltage applications and components of spark-gap gas switches, which serve as an important overall system controller for remote and synchronous control. Specifically, acceleration voltages of up to 800 kV can be generated. By using the Blumlein pulse forming line (Blumlein PFL), the underdamping sinusoidal waveform generated via the Marx generator maintains the applied maximum acceleration voltage. This proceeds as a square pulse and aids the electron beam to accelerate favorably. Simultaneously, 1500 liters of deionized water is contained inside the Blumlein PFL to ensure that the relative permittivity is 78 and specific resistance is maintained at approximately 18 MΩ·cm. This ensures that there is no insulation breakdown problem. The red velvet cathode in the MILO circuit shown in Fig. 1-(a) has a very low concentration of impurities in the plasma state in vacuum. Hence, the probability of a break-down inside the vacuum is very low. Self without external magnetic field characteristic of the MILO circuit It is characterized as a very advantageous material for forming magnetization. After the formation of field emission on the surface of velvet cathode through the MILO circuit, RF oscillates through the beam–wave interaction in the

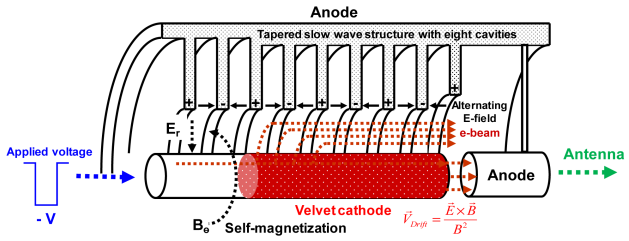

FIGURE 2. MILO circuit (synchronism condition: $V_{beam} = V_{RFphase}$).

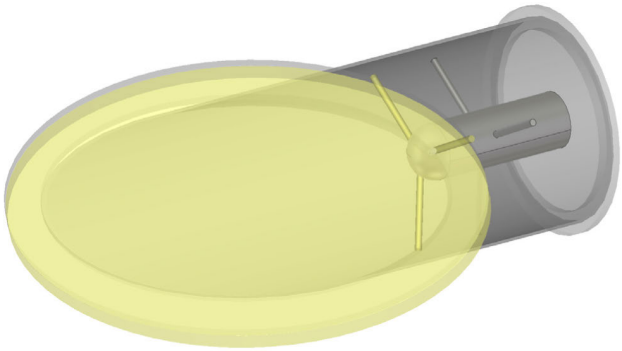

FIGURE 3. 3D modeling of a vlasov antenna.

several cavities between a relativistic electron beam and slow wave structure. Simultaneously, the resonant frequency is determined (approximately 1.15 GHz) due to the specially designed cavities and its dimension characteristics, and it can radiate to the exterior in the air while intactly propagating or converting a specific mode through the antenna.

As shown in Fig. 2, MILO is composed of several continuous resonators in a vacuum coaxial diode composed of a cathode and an anode. In Fig. 2, when a negative input pulse is transmitted from the left, electrons flow through the central conductor and are emitted through the cathode. At this time, this flow of electrons creates a magnetic field in the direction of rotation, and if the current is sufficiently high, then it acts together with the electric field in the given radial direction to form E $\times$ B drift motion in the axial direction. Eventually, the electrons do not reach the anode and flow in the axial direction, which is termed as self-magnetic insulation. This electron beam is decelerated or accelerated in this manner by a specific mode of the resonator. Specifically, this corresponds to the π mode with a phase difference of π for each vane. If the speed of the electron beam is similar to the phase speed of this mode, then an electron beam bunch is formed in this manner, and this bunch releases energy to generate strong coherent radiation (synchronism condition).

B. VLASOV ANTENNA

The fundamental mode of electromagnetic waves generated from MILO circuit in Fig. 2 is either TEM or TM_{01} mode. In the electric field distribution, the central electric field is zero. This implies that when the electric filed is analyzed with a three-dimensional radiation pattern, the radiation proceeds in a donut shape. Hence, it is impossible to reach a desired target when the electromagnetic waves are radiated in air through the antenna. To overcome this limitation in this study, an antenna design with a mode conversion function to transform TM_{01} mode to TE_{11} mode, in which the electric field is the highest in the center, is required. It is necessary to design an optimized design via computational simulation studies. Based on Fig. 3, the actual fabrication was conducted by securing the data from the simulation.

As shown in Fig. 3, the Vlasov antenna is basically composed of a circular waveguide and can be used with a reflector or a lens that can provide a phase difference according to the application. The Vlasov antenna cuts the end of the circular waveguide at a certain angle and connects the end with a polyethylene-based lens. Additionally, it interacts with the low-speed structure in the MILO circuit, exhibits a resonant frequency, converts the mode of the electromagnetic wave that travels, and plays an important role in radiating the electromagnetic wave in air via the lens. Given that the Vlasov antenna operates as an antenna using the cross section of the waveguide, it is generally suitable for cases with large-diameter waveguide, which is widely used in L-band with a relatively low operating frequency or resonant frequency. Additionally, the Vlasov antenna, which has a small aperture when compared to the wavelength according to frequency, exhibits the advantage of reducing the area of electric field distribution because of its relatively low gain. However, given that electromagnetic waves radiate in a tilted propagation direction, they exhibit frequency dependence due to elliptically polarized light. This serves as a disadvantage for the Vlasov antenna. Furthermore, it has the characteristic of a narrowband antenna, in which the direction of the antenna should be changed by the resonant frequency because the direction and tendency of the radiation pattern vary according to the operating frequency.

Based on the modeling-based design optimization data in Fig. 3, the radiation pattern in the air was predicted and analyzed via simulation. In Fig. 4, the center is 0° in the vertical plane, and the angular width is 100°. With respect to the horizontal plane, the center is 45° and angular width is 38°. The three-dimensional radiation pattern can be expected as elliptical.

Based on the aforementioned results, a Vlasov antenna is manufactured and externally configured for a cold test as shown in Fig. 5. With respect to the combination of the separately manufactured mode converter and Vlasov antenna, the operating frequency of MILO is 1.15 GHz, the input of the mode converter is TEM mode, and the output corresponds to the circular waveguide in TE_{11} mode, which is converted by the mode converter. The measurement items of the combination of the mode converter and Vlasov antenna include reflection coefficient, radiation pattern, and gain. Given that the measurement of the reflection coefficient of the antenna should be obtained independently of the surrounding environment, the measurement cable of the calibrated vector network

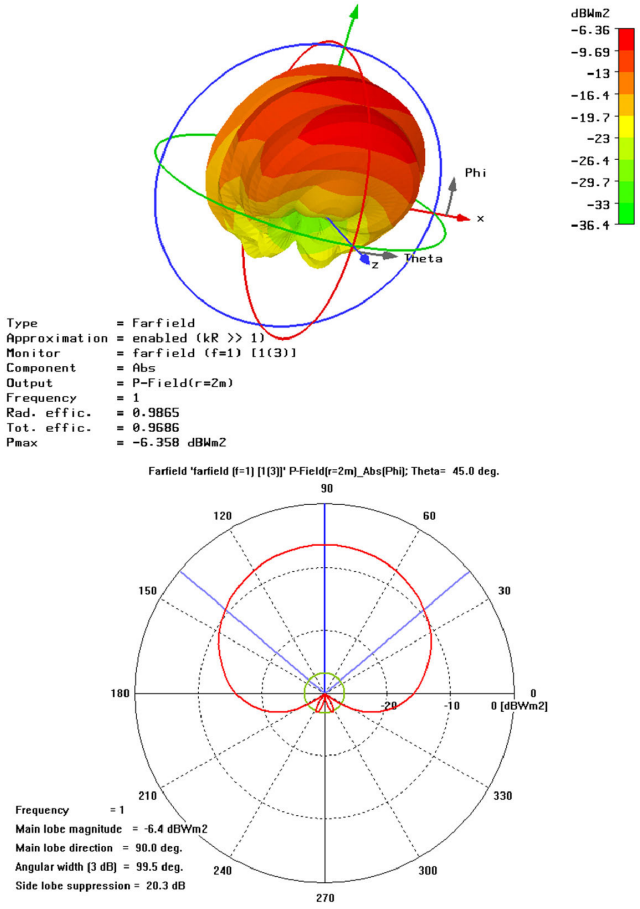

FIGURE 4. Simulation (CST) results of a vlasov antenna.

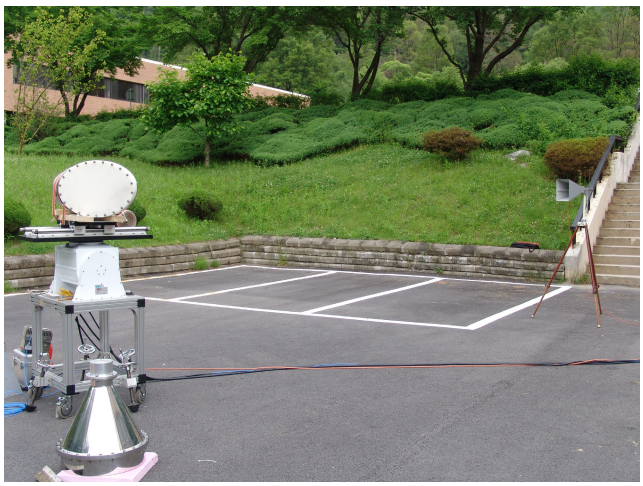

FIGURE 5. Cold test of a vlasov antenna.

analyzer should be fixed to eliminate the phase change error due to the cable. Hence, it is necessary to install a radio wave absorber around the cable to reduce the influence of the signal reflected on the ground or surrounding objects. To measure the radiation pattern and gain, a long-distance measurement method was used. Given that the distance measurement is

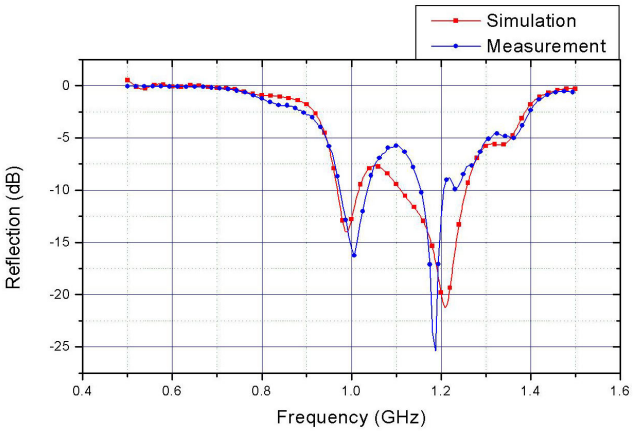

FIGURE 6. Cold test result of vlasov antenna: reflection coefficient.

performed by only using θ- and φ-direction glottal gates, as there is no radial component in the spherical coordinate system, the measurement process is simple. However, a location that satisfies the distance condition is required. In the measurement method, the radiation pattern is measured via an antenna operating in the same frequency band, and the gain is calculated by comparing the relative value with the data measured under the same conditions with an antenna with a known gain. Hence, the radiation pattern is normalized. Given that the cut-off frequency of the mode converter and antenna assembly in the cold test is 1 GHz, applying to the formula of $2D^2/\lambda$, which is a long-distance condition, is about 2 m.

First, the reflection coefficient of the Vlasov antenna was measured. The result is shown in Fig. 6. The reflection coefficient measurement result showed an error of approximately 4 dB when compared to that of the design case. Fig. 7 shows the result of the cold test measurement in terms of the radiation pattern and antenna gain. The radiation pattern and gain were measured at 1.0 GHz and 1.2 GHz with the operating (resonant) frequency of 1.15 GHz as the center. The results in Fig. 7 show that the gain of the Vlasov antenna is maximum at the center with an approximate value of 10 dB. This shows that the mode conversion was performed correctly from TM_{01} to TE_{11}. Hence, the targeting is expected to function accurately on the desired object.

The main beam formation angle was compared with the design value and experimental value for each frequency in Table 1.

III. EXERIMENTAL PERFORMANCE RESULTS

A. PERFOMANCE EXPERIMENT FOR THE MILO SYSTEM

As shown in Fig. 8, the MILO system was fabricated and the experimental configuration for performance test was completed. Fig. 8-(a) shows the overall MILO system, in which the Marx generator and Blumlein PFL are assembled with a Vlasov antenna that modulates electromagnetic waves and radiates them outward. Fig. 8-(b) shows the cathode that covers the velvet. Hence, the velvet is mounted on the surface of the anode to facilitate the emission of electrons.

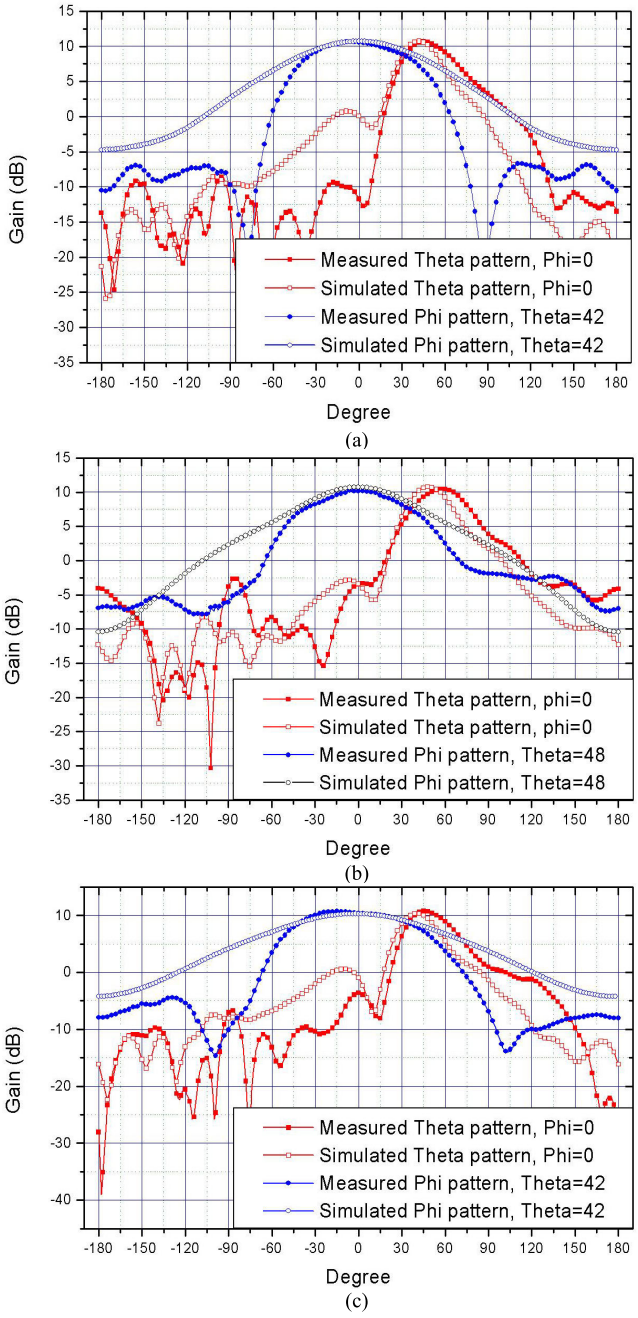

FIGURE 7. Distributions of radiation pattern and gain for vlasov antenna; (a) 1.15 GHz, (b) 1.0 GHz, and (c) 1.2 GHz.

The output power facilitates the emission of electrons as the work function value is lowered when compared to the material of the existing cathode by mounting the velvet. Finally, a dielectric material, such as velvet, was attached to the surface of the cathode to generate high-quality electron beams on the surface of the cathode. This was performed using a shape that facilitated uniform electron emission by forming fine gas columns. Based on these results, the weakness of MILO, which has a relatively low output conversion efficiency of 10% or less, can be compensated to some extent.

TABLE 1. Main beam forming angle from the cold test of vlasov antenna.

Frequency	Design		Measurement (cold test)	
	θ	φ	θ	φ
1.0 GHz	49	0	59	-4
1.15 GHz	42	0	45	-6
1.2 GHz	39	0	46	-15

When connected to each other, as shown in Fig. 8-(c) and Fig. 8-(d), the velvet cathode (to which the velvet is attached) and central anode are positioned at a certain distance. This enables mode-converted radiation of electromagnetic waves under a resonant frequency mode due to the beam–wave interaction from the cathode to the central anode via the Vlasov antenna. This leads to a circularly symmetrical mode via the circularly symmetrical central anode when the monopole's electromagnetic field affects the inner core conductor under the influence of the separation distance between the central anode and velvet cathode, which has the characteristics of an inner conductor.

Fig. 9 shows the performance test results of the MILO system. In Fig. 9-(a), the applied acceleration voltage can be approximated as 600 kV considering the full width at half maximum, and the RF output power is observed at 3- GW level. Furthermore, the range for the beam current can be calculated by using a diode impedance of 14 Ω. In Fig. 9-(a), the maximum beam current is observed approximately at 40 kA. In the study, the beam current was measured with a B-dot probe. Fig.9-(b) confirms the oscillation frequency via fast Fourier transform (FFT) operation based on the RF power signal measured by the power meter. Furthermore, it was confirmed that the resonance frequency for the main mode oscillates at 1.15 GHz. As for the phenomenon that the RF pulse is shorter than the applied beam voltage in Fig. 9-(a), the anode plasma generates an ion flow toward the cathode. As these ions neutralize with electrons near the cathode, they reduce the space charge limitation, and the emission current increases. An increase in emission current leads to strong and fast insulation and prevents the growth of 5/6 π mode, which competes with π mode in the early stage of the diode operation. This leads to a reduction in the RF pulse when compared to the length of the applied voltage pulse [21].

Fig. 10 shows the database obtained through hundreds of experiments to secure reliability and reproducibility, which are indicators of the performance guarantee of the MILO system. Fig. 10-(a) shows the RF output power with respect to the applied beam voltage, and Fig. 10-(b) shows the power efficiency with respect to the applied beam voltage. In both plots, as the applied beam voltage increases, the predicted values of simulation and experimental results tend to differ. This is related to the phase velocity of electromagnetic waves wherein the beam¬–wave interaction should be considered as the applied beam voltage increases. This is closely related to the axial mode competition with respect to the formation of

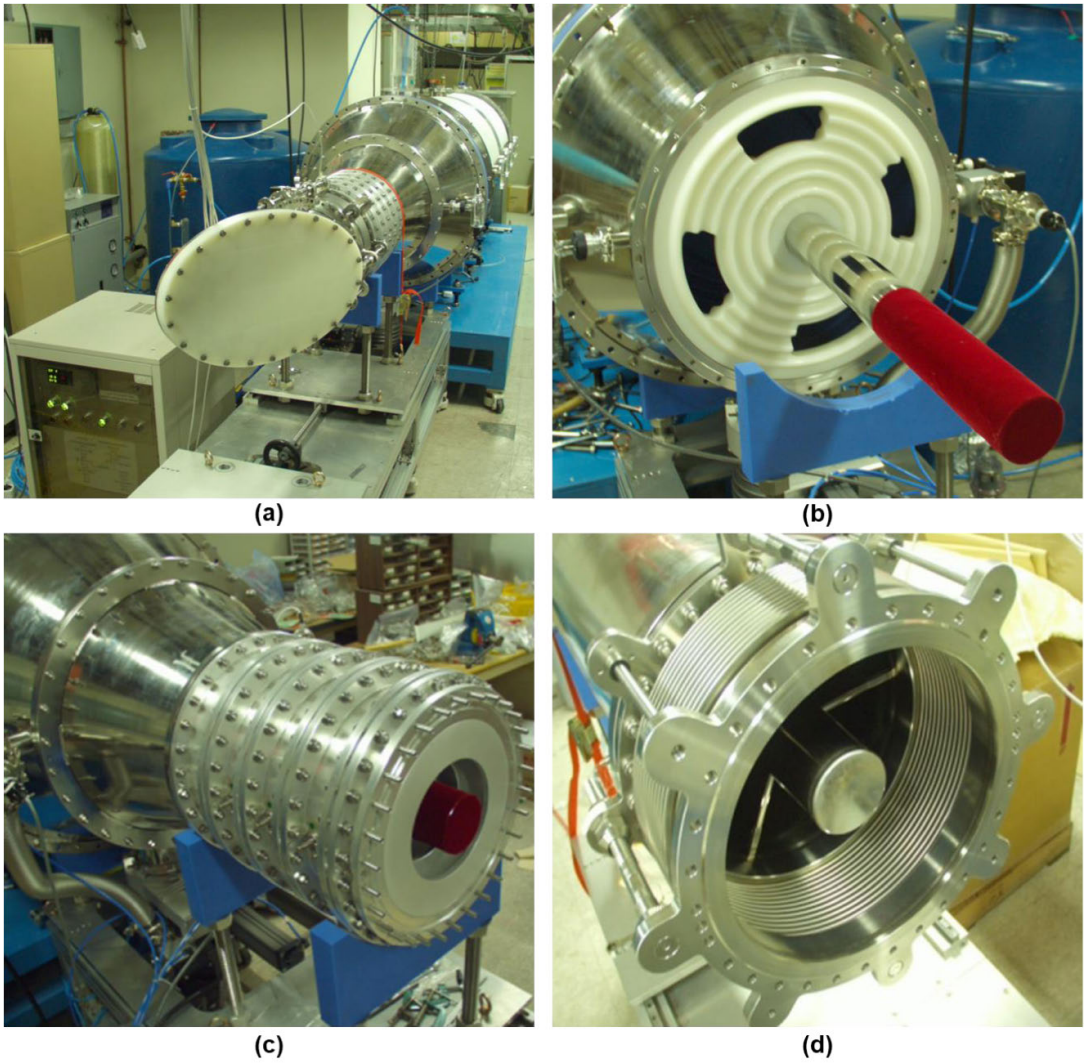

FIGURE 8. Fabricated MILO system; (a) MILO with vlasov antenna, (b) Velvet cathode, (c) Cavities in MILO, and (d) Central anode with flexible coupling.

anode plasma. This phenomenon tends to decrease the power efficiency as the applied beam voltage increases [21].

B. EFFECTIVENESS OF ELECTRONICS EXPOSED TO EMP WITH MEASUREMENT

Previously, the performance of the EMP was verified via the experimental results of the MILO system. Subsequently, we analyzed the effect on electronic devices via GW-class electromagnetic pulses generated by the MILO system. Then, by setting the experiment shown in Fig. 11, it is easy to analyze the effects under the EMP exposure condition on electronics such as mobile phones. In Fig.11-(a), a mobile phone is placed as a sample electronic device, and a D-dot probe is used to measure the electric field in a position close to it is configuration. In this experimental system, various calibration methodologies have been suggested in other experimental areas in advance and numerous experiments have been performed. Furthermore, a database has already been established based on experimental data obtained through HPM sources with the exception of the MILO [13]. Fig.11-(b) confirms the degree of electrical damage to a mobile phone, which serves as a sample for analyzing the effects of electronic devices before and after the experiment. The mobile operated properly before the experiment. However, after the experiment, even when the power was turned on, only a white screen was displayed. Subsequently, the power was turned off and the device did not work at all. This can directly confirm that the function of the electronic device was disabled due to the permanent damage. Given the limitations of the experimental space and safety, environmental conditions were not secured for outdoor testing. Furthermore, the exposure range of the electronic devices was at a distance of approximately 2 m from the center of the Vlasov antenna. This was set in a manner similar to the distance condition of 2 m based on the law of $2D^2/\lambda$ mentioned above.

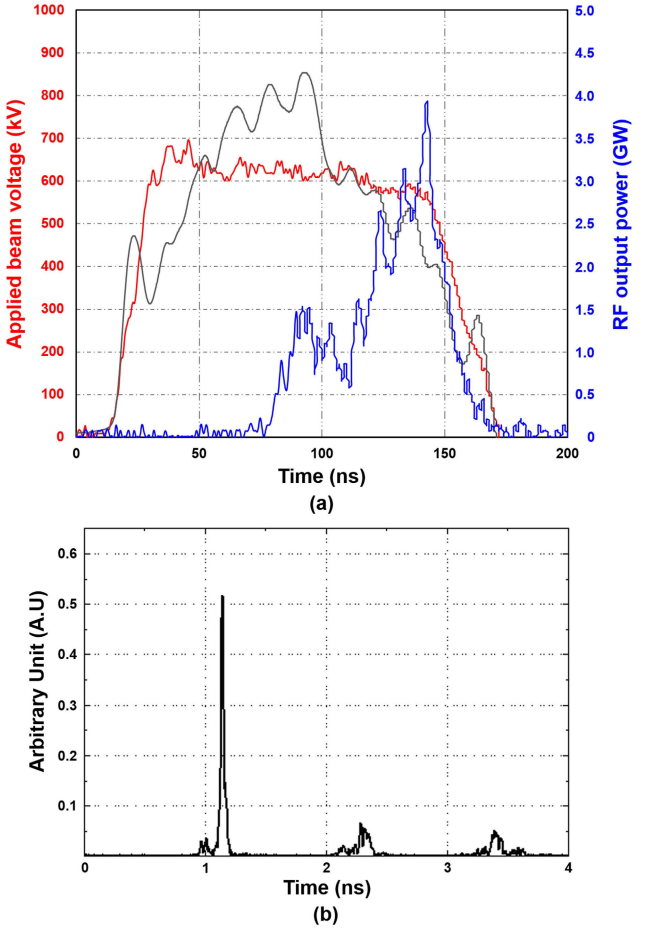

FIGURE 9. Hot test result of the MILO system; (a) The pulsed waveforms of applied beam voltage (red line), RF output power (blue line), and beam current (gray line); (b) Operating frequency through FFT (fast fourier transform).

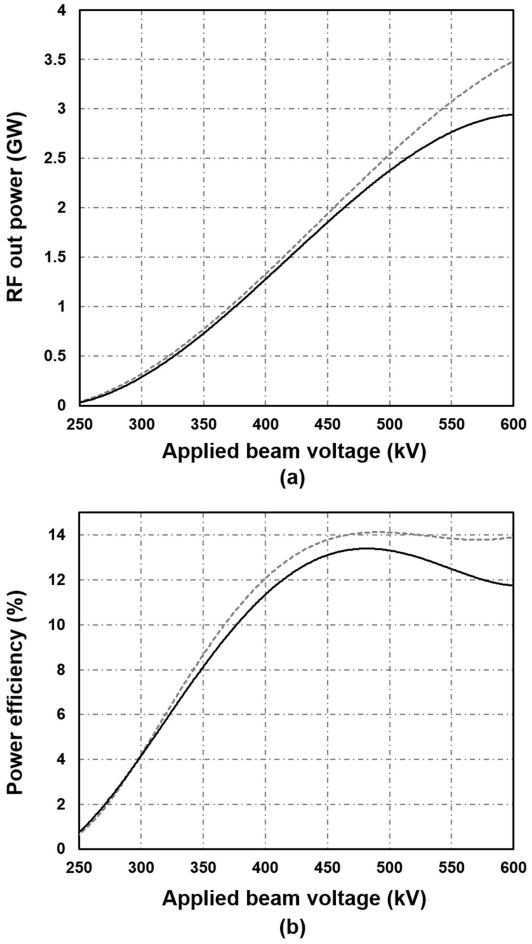

FIGURE 10. Arrangement of data; (a) Applied beam voltage vs. RF output power; (b) Applied beam voltage vs. power efficiency, (the dotted line shows the computational simulation result, and the solid line denotes the fitting of the experimental results).

As shown in Fig.11-(a), in the actual hot test, the value of the electric field radiated into the air by the TE_{11} mode electromagnetic wave was measured through the Vlasov antenna of the MILO system via the D-dot probe, which was positioned 2 m away. The results can be confirmed through Fig.12. The theoretical and simulation prediction values were also compared. Although there was a slight difference in the electric field values, the overall trend showed no changes. The measured value of the electric field of electromagnetic waves, which were radiated from the MILO system in a far-field condition, was a few kV/cm and did not reach the breakdown level in air (30 kV/cm). However, this range of the electric field can permanently damage electric devices and can lead to temporary operation errors (100 V/m to 10 kV/cm) [13].

The distribution of the electric field in the MILO system can be predicted via CST simulation. As shown in Fig. 13, the electric field distribution around the end of the MILO circuit and the window of the Vlasov antenna can be verified. At position (a) in Fig. 13, the electric field value is approximately 180 kV/cm, which is very high because it is a region of metal surface breakdown in vacuum. The electric field near the window ranges from 26.8 kV/cm to 33.2 kV/cm. In this condition, given that air-breakdown can occur in air, SF_6 gas (2–3 bar) is injected, as shown in the lower left part of Fig. 11, to reduce the experimental risk.

By estimating the power density at a distance of 2 m under the far-field condition, 3 GW of electromagnetic wave radiated RF power can be expected to exhibit a maximum value of 52.65 kW/cm^2. This provides the basis for estimating the actual power density under the long-distance radiation condition by checking the gain and radiation pattern distribution in the cold test result of the Vlasov antenna mentioned in Section II-B.

IV. APPLICATION TO AN HPM SOURCE MOUNTED ON A MOBILE VEHICLE BASED ON PERFORMANCE

The performance test of the MILO system was confirmed based on the results of previous studies and the results mentioned above. To apply the system in the defense industry, it should be mounted on a mobile vehicle on land for practical applications. A practical example of such an application is shown in Fig.14. Specifically, in Fig.14-(a) – (d), the right

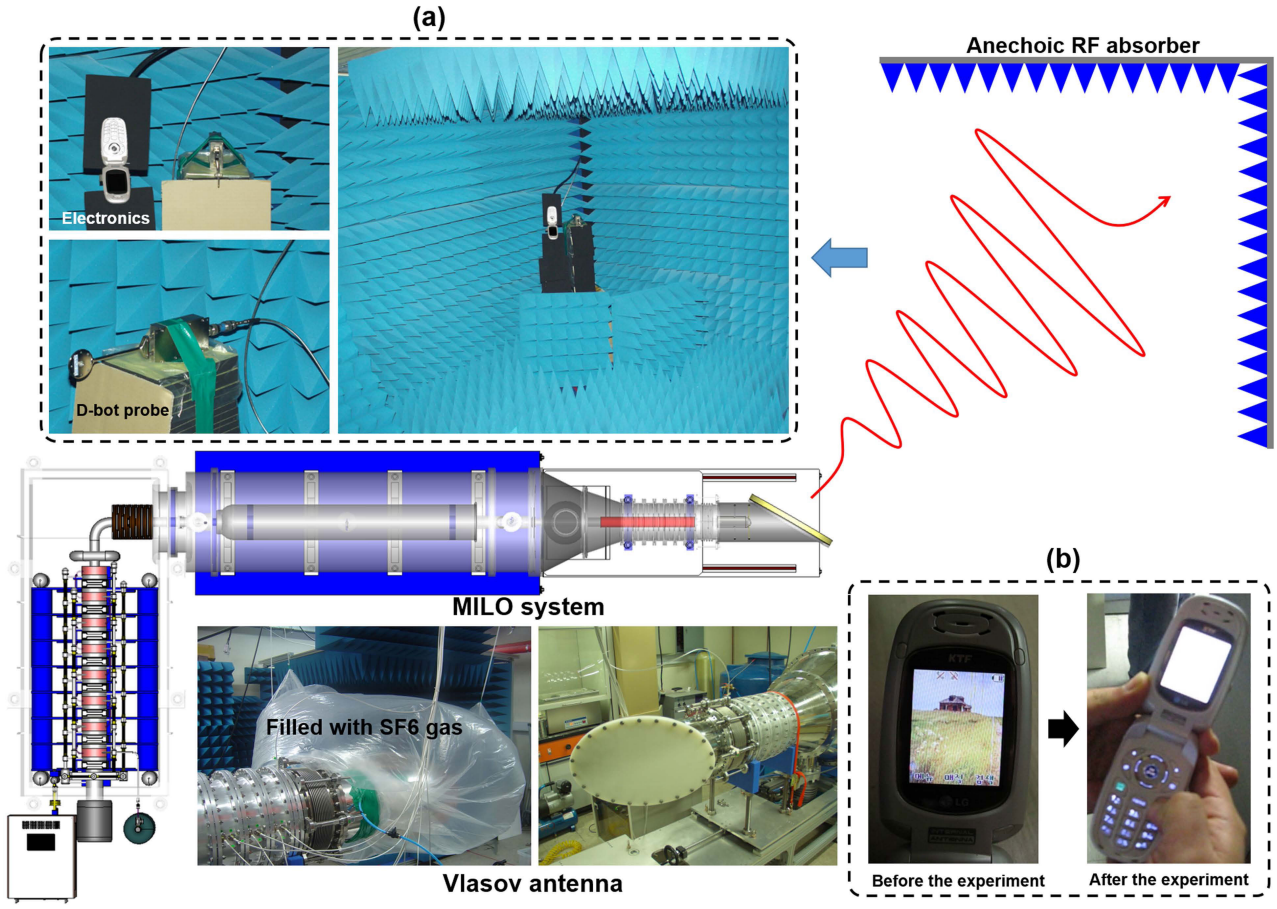

FIGURE 11. Experiment to test the effectiveness for electronics exposed to EMP in the MILO system; (a) Measurement of electric fields through D-dot probe; (b) Verification of electrical damage on electronics (a mobile phone).

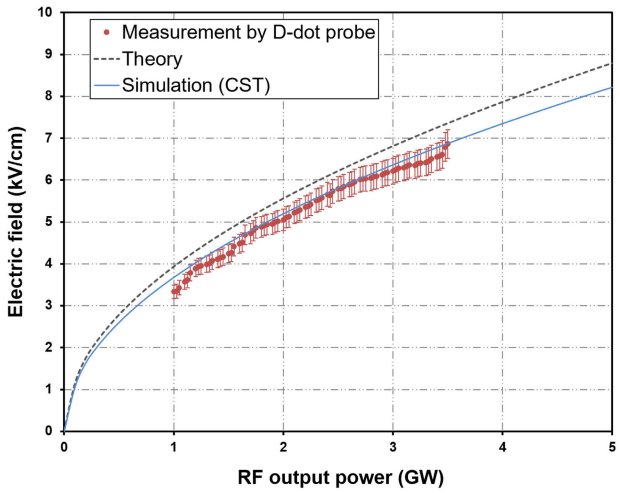

FIGURE 12. RF output power vs. electric field; The electric field values measured through the D-dot were compared with theoretical calculations and simulation results. The range of the measured electric field was considered within the error range of approximately 5%.

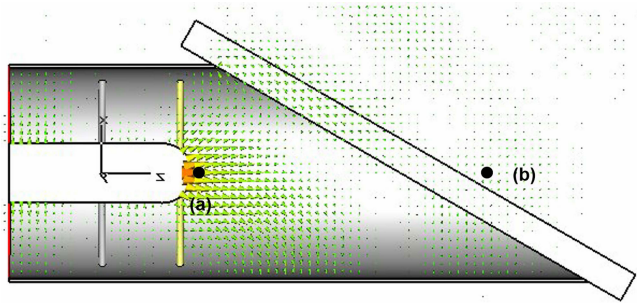

FIGURE 13. The expectation of electric fields through simulation (CST) for vlasov antenna in MILO system; (a) The maximum electric field = 180 kV/cm, the electric field range on the window of vlasov antenna = 26.8 kV/cm to 33.2 kV/cm.

side view shows that the control system is included, and the top view shows the overall configuration at a glance.

A directed energy weapon (DEW) is a weapon system that instantaneously radiates concentrated energy in a specific direction to disrupt or overload enemy electronic equipment. To design and determine the performance of this type of directed energy weapon, the analysis of the effect on the target is one of the important factors that should be considered.

The directed energy weapon of EMP based on the MILO system, proposed in Fig. 14, applies transient voltage and current to an electronic equipment with a semiconductor device, as shown in Fig. 15, to induce temporary abnormal conditions, arc discharge, and spark generation. The system

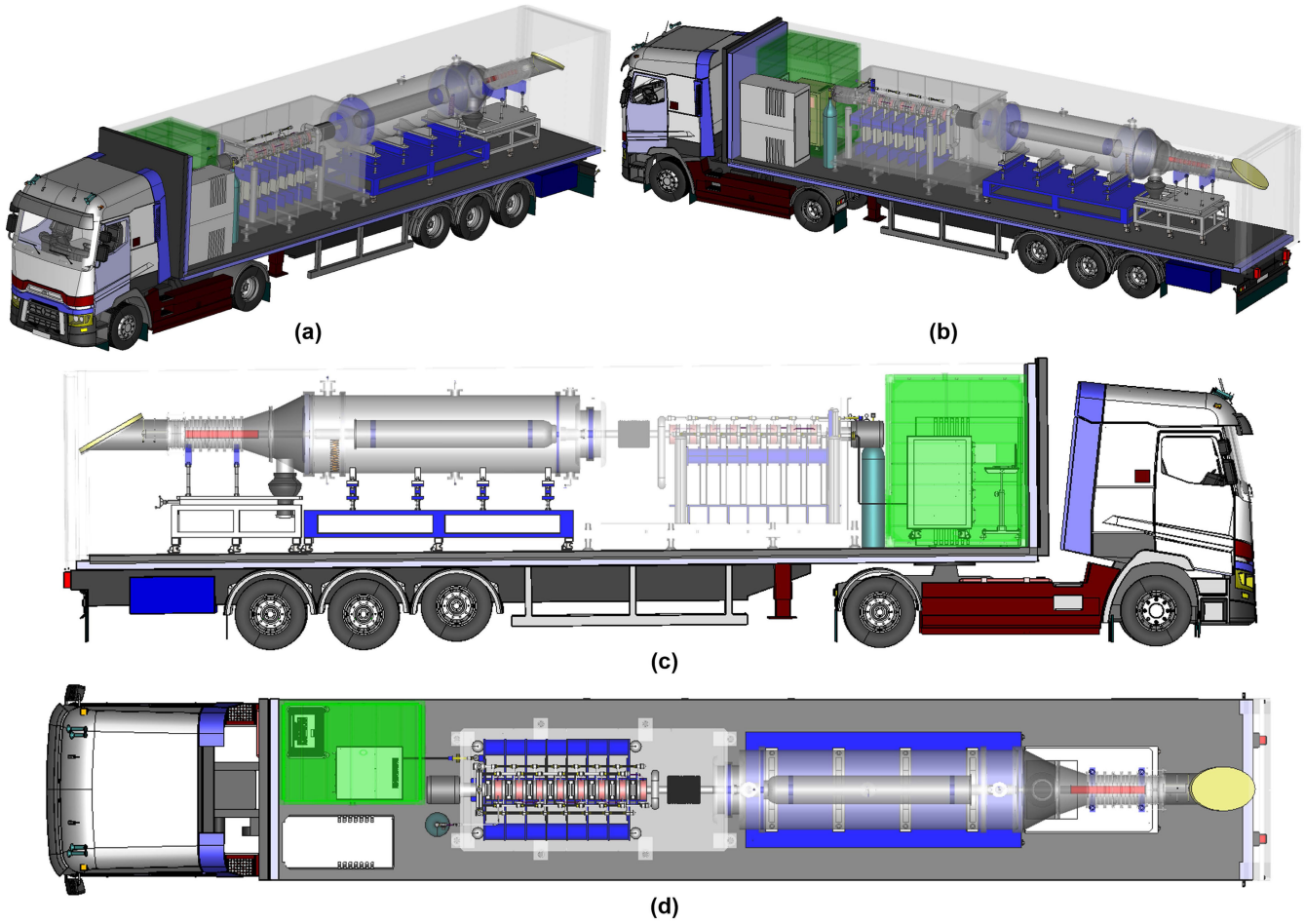

FIGURE 14. Potential application for defense industry based on the MILO system mounted in a movable vehicle (3D modeling); (a) 3D modeling view on the left side, (b) 3D modeling view on the right side, (c) right side view, and (d) top view.

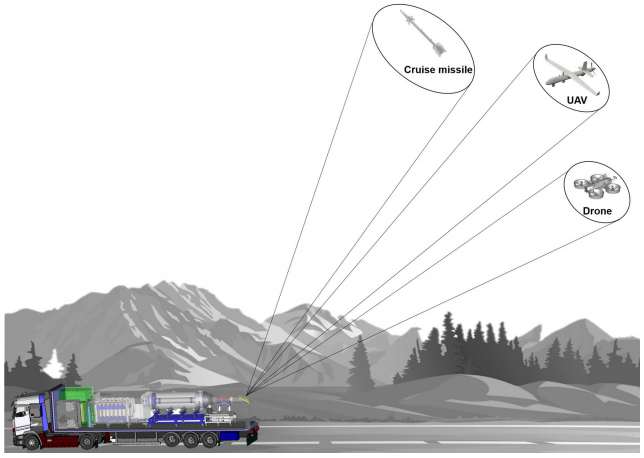

FIGURE 15. Conceptual outline of directed energy weapons.

can potentially incapacitate the target (cruise missile, drone, UAV, etc.) by causing permanent damage to the semiconductor device. The effects of directional energy weapons can be divided into 4 categories as shown and defined in Table 2.

TABLE 2. Classification of HPM-EMP effectiveness.

Classification	Damage effectiveness
Upset	Temporary abnormal state Return to normal state when the cause is removed
Lock-up	Temporary abnormal state Return to normal state after electrical reset when the cause is removed
Latch-up	Permanent damage due to electrical faults
Burn-out	Permanent damage due to physical defects

To obtain the effect of such a directed energy weapon, electromagnetic waves above a certain level must be delivered to the target, and it is known that the average power density that should be applied to the target corresponds to several mW/cm^2 (tens of W/m^2) or more. To realize the effectiveness of directed energy weapons, it is necessary to derive the required performance for each component of the weapon system [39]–[41].

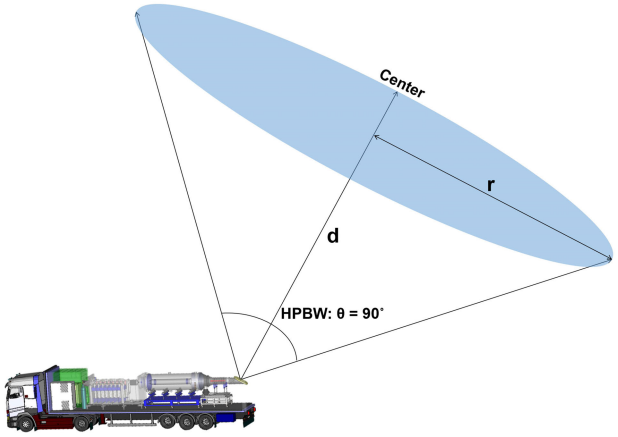

FIGURE 16. HPM-EMP effectiveness area with respect to distance (d) in a directed energy weapon (DEW).

Based on the conceptual diagram in Fig. 16, the electric field for the effective radius with respect to the distance is obtained via the CST simulation for the Vlasov antenna (Table 3). Furthermore, the power density applied to the potential target located in the actual effective radius is obtained and analyzed (Table 4).

TABLE 3. Comparison of simulation with the theory of electric field.

Distance (km)	CST simulation		Theory (Friis formula)	
	HPBW (kV/m)	Center (kV/m)	HPBW (kV/m)	Center (kV/m)
1	1.0800	1.3100	1.1225	1.3616
2	0.7300	0.9400	0.7937	0.9628
4	0.4800	0.6200	0.5613	0.6808
8	0.3100	0.4200	0.3969	0.4814

TABLE 4. Comparison of simulation with the theory of power density.

Distance (km)	CST simulation		Theory (Friis formula)	
	HPBW (W/cm^2)	Center (W/cm^2)	HPBW (W/cm^2)	Center (W/cm^2)
1	165.8	236.1	167.09	238.71
2	40.8	58.8	41.77	59.68
4	9.8	14.1	10.44	14.92
8	2.2	3.2	2.61	3.73

The electric field and power density simulation is performed by irradiating electromagnetic waves of 3 GW of the RF output power for the proven performance generated in the MILO system. Then, the electric field and power density are measured within the effective radius for half power beam width (HPBW) 90° at various distances (1 km, 2 km, 4 km, and 8 km). The maximum/minimum power density is generated at the center/edge of the effective radius, and the difference between the maximum and minimum is 3 dB. This corresponds to a beam width of 3 dB of the antenna radiation pattern. Table 3 shows the comparison between the simulation results and those obtained via the theory of the electric field generated from the radiated electromagnetic wave based on the radiation distance (d) of the Vlasov antenna. As expected, the electric field appeared to be effective for the target at approximately several kV/m. Within the range of this type of an electric field, electronic devices can potentially affect temporary functional disturbance and permanent damage. Similarly, Table 4 shows the comparison between the simulation results and theory for the power density of radiated electromagnetic waves based on the radiation distance (d) of the Vlasov antenna. It is formed in the range of several to several hundred W/cm^2 based on the distance and shows the performance is sufficient to seriously affect electronic devices.

As the incident electromagnetic wave from Vlasov antenna, in Fig. 16, radiates, an effective cone zone vulnerable to EMP can be formed. In this condition, the radius of the effective area that can lead to temporary malfunction or permanent damage to an electronic device due to the influence of intentional EMP from the generated HPM can be predicted using Eq. (1). In the equation, r denotes the radius of the covered area, and θ denotes the beam angle. However, θ is based on HPBW as mentioned earlier [42].

$$r = d \tan\left(\frac{\theta}{2}\right) \tag{1}$$

In Fig. 16, HPBW θ is 90°. Hence, the calculation of the radius of the covered area can be easily calculated as shown in Table 5.

TABLE 5. Calculation of the radius of the covered with respect to d based on HPBW.

d	The radius of coverage area			
	1 km	2 km	4 km	8 km
θ = 45°	1 km	2 km	4 km	8 km

As a feasible technique for causing damage or destruction of electronic and other equipment, HPM can damage many possible targets, including computers, communication systems, aircraft, UAVs, drones, shipboard, land vehicles, explosive, detonators, and other digital equipment.

V. DISCUSSION

In the previous sections, the technology and measurements for intentionally generating EMP based on an HPM source were described. Based on the experimental studies in this paper, we secured a database on the electric field and power density of radiated electromagnetic waves. Based on the results, the technology is at a level that can neutralize potential military equipment, including temporary malfunction and permanent damage to objects based on electronic devices at a distance.

In this section, the damage to electronic devices due to intentional EMP exposure from HPM sources to mobile

objects based on electronic devices and military equipment are described in relation to protection technology.

In modern social infrastructure, various types of information and communication equipment are being operated in conjunction with each other based on the demand for artificial intelligence (AI) technology corresponding to informatization and automation technology. This can not only cause chaos, but it can also spread throughout the national security system and can cause enormous damage. Specifically, given that these effects can spread to almost all electronic equipment, including power grids and communication networks, it requires a significant amount of time to recover after an accident.

Recently, as the perception of EMP protection technology has changed, there is an increasing interest in this technology as a national project. Hence, advanced countries in defense have recently become aware of the serious threat posed by these high-power electromagnetic waves, and thereby are investing significant amount of effort for building related protection facilities. However, these types of projects are experiencing difficulties, such as excessive costs for building protection facilities, due to the lack of related technologies and insufficiency in localization of the protection devices. High-altitude nuclear electromagnetic waves and high-power non-nuclear electromagnetic waves differ from each other in field source, spatial coverage, time-domain characteristics, frequency spectrum, and exposure field strength. Therefore, the effects are different, and the protective measures against them also differ. Specifically, with respect to the international standards and standardization applied to HPM-based EMP protection technology in the defense field, most of the equipment used for military purposes is designed to satisfy the electromagnetic compatibility (EMC) technology standard, which is similar to the MILSTD-461F standard. Other test items, including frequency ranges and test levels, are applied. While most of the army's ground equipment is not subjected to RS105 among test items (CSI16, RS105) related to high-power electromagnetic pulses, it is subject to RSI03 for radiation immunity in the 2 MHz to 40 GHz frequency band. Therefore, the army's ground equipment is designed to withstand an electric field strength of 50 V/m in the frequency band of 2 MHz to 40 GHz, and it varies based on the frequency according to the CS116 test item. However, it is designed to withstand a damped vibration wave of up to 10 A. Therefore, the field strength and induced current directly exposed by high-power electromagnetic waves are much higher than the radiation immunity and conduction immunity of the army's ground equipment. This can lead a fatal obstacle to mission performance. Additionally, in recent years, civil equipment has been widely used in major military facilities as commercially available off-the-shelf (COTS) equipment. Hence, some of these civilian equipment are not subject to electromagnetic compatibility standards and they often exhibit a significantly lower level of electromagnetic immunity than that of military standards. Therefore, it is necessary to set an appropriate protection target via a detailed analysis of the protection target facility [44], [45].

The performance and test method must be equipped with ground-based and mobile protection facilities against high-power electromagnetic waves. These parameters are stipulated in comparative detail in the military standard MIL-STD-188-125-1/2 [47], [48]. Fig.17 shows the electromagnetic shielding effect performance required according to the military standard MIL-STD-188-125-1/2 [46]. However, this standard is for the protection of ground-based C41 equipment, and there is a limit to its application to private facilities as well as concrete structures and underground bunkers.

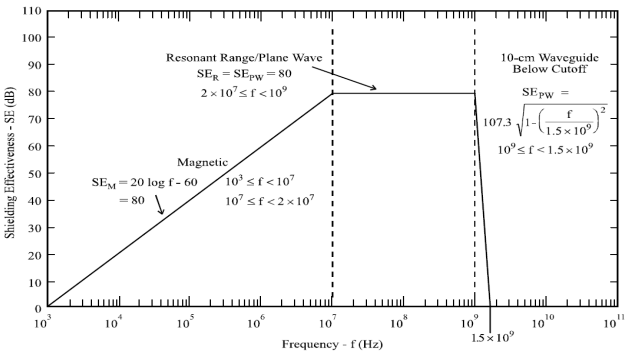

FIGURE 17. Minimum HEMP shielding effectiveness requirements (measured IAW procedures) [46].

The principles used in setting protection goals are as follows:

$$\text{Protection Target (dB)} = \text{Threat Level} - \text{Vulnerability Level} + \text{Safety Margin} \quad (2)$$

In this equation, the safety margin should be more than 6 dB according to the military standard MIL-STD-464C [48]. For example, by assuming that the field strength generated by high-power electromagnetic waves is 65 kV/m, the electromagnetic shielding effect required to protect military equipment with a radiation immunity of 50 V/m is based on Eq. (2). Hence, the same result, as that in Eq. (3), can be obtained [49] as follows:

$$SE\ (dB) \geq 20 \log \left(\frac{65kV/m}{50V/m} \right) + 6\,[dB] \approx 68dB \quad (3)$$

Therefore, the result of Eq. (3) can be protected with a protection facility with the same performance as Fig. 17. However, if a commercial off-the-shelf product with a radiation tolerance of 3 V/m is included in the system, then the required electromagnetic wave shielding effect can be expressed in Eq. (4) as follows:

$$SE\ (dB) \geq 20 \log \left(\frac{65kV/m}{3V/m} \right) + 6\,[dB] \approx 93dB \quad (4)$$

Therefore, there is a limit to realizing complete protection with a protection facility according to the military

standard MIL-STD-188-125-1I2. Although the electromagnetic wave shielding effect is often emphasized in the performance of EMP protection facilities, the high-power electromagnetic pulses that are induced in the power lines and signal lines and transient signal that can enter the facility through the point of entry (PoE) are more important performance metrics. It can be seen that it depends on how to effectively reduce the coming. Therefore, the military standard MIL-STD-188-125-1/2 stipulates not only the requirement for electromagnetic wave shielding effect, but also the pulse current injection (PCI) test and continuous wave immersion (CWI) test. A short circuit injection of up to 5 kA for various types (inter-site, intra-site) of power lines, audio/data lines (inter-site), control and signal lines (intra-site), conduit pipes, and RF antenna lines for pulses is specified. Furthermore, a maximum residual internal stress of 10 A or less under different load conditions is specified. More details on this are available in the military specification MIL-STD-188-125-1/2 [46], [47].

When considering the performance specifications of the MILO system again, if electromagnetic waves of peak RF exceed 3 GW of RF output power and are radiated into the air, then the range of the effective radiated electric field with respect to distance can be estimated using the results of Table 3 and Table 4. If 68 dB is attenuated and shielded by applying the result of Eq. (3), then the electric field of radiated electromagnetic waves is distributed in the range of 130 – 155 V/m at d = 1 km and in 60 – 90 V/m at d = 2 km. It is in the range of V/m. This is within the range of 30 – 70 V/m, where temporary system malfunctions occur, and in the range of 150 V/m, where permanent hardware damage and system software damage occur. When viewed as an illusion of power density, it is included in the level of 60 – 300 mW/cm^2. This can lead to malfunction and damage to electronic devices [13], [50]. However, the distance is in the range of 1 – 2 km, and it is estimated that the effective distance and effectiveness of the electromagnetic waves are reduced by 1/4 when compared to the case where the protection system is not installed.

In the case of applying a protective facility and metal grid structure, as shown in Fig. 17, a shielding effect of 70 – 80 dB or more can be obtained in general. This leads to a potential design for effective protection. However, in the case of a metal grating structure, the interval between the periodically arranged grating structures is related to the wavelength of electromagnetic waves. Hence, there is a limit to the shielding effect for high-frequency signals of several hundred MHz or more. Therefore, there is a protection limit even if the EMP protection system is built under the radiated electromagnetic wave condition of a system that can oscillate the RF output of the GHz class GW based on the HPM source such as MILO. Additionally, even if EMC shielding is applied to aircraft, such as cruise missiles, UAVs, and drones, it is difficult to prevent the influence due to the presence of metal antennas and structural apertures. Hence, even if a protection system is built through electromagnetic shielding with a GW-level of GHz ultra-high frequency electromagnetic wave radiation condition, it can inevitably be affected by a risk factor for malfunction or damage. It is evident that in the private sector, RF shielding facilities of 120 dB or more can be constructed. However, military equipment is designed with a limit of 70 – 80 dB.

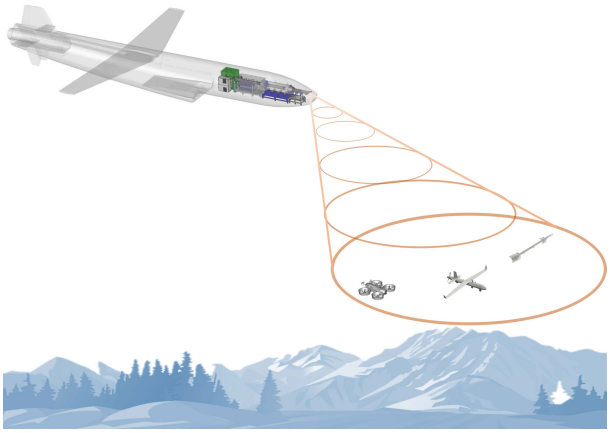

FIGURE 18. Conceptual diagram of an aircraft equipped with MILO system for anti-drone applications.

Finally, for high-power electromagnetic wave protection, a comprehensive approach, including countermeasures at the protection facility boundary, countermeasures at the overall system level, and countermeasures at the equipment level, is required. These approaches include the concept of the zone of space that should be protected, the selection and separation and routing of cables that can be exposed to high-power electromagnetic pulses, methods of shielding and filtering shielded spaces, and use of devices to detect transient electromagnetic fields and transiently conducted signals. These countermeasures typically require electromagnetic wave shielding, power line and signal line filters, and non-linear countermeasures and non-linear countermeasures against transient currents and voltages. To prevent the radioactive coupling of high-output electromagnetic waves, protection facilities should exhibit appropriate electromagnetic wave shielding effects and various structural intrusion points countermeasures. To suppress conductive interference, high-power electromagnetic wave countermeasure power lines and signal line filters as well as lightning surges are required. Specifically, countermeasure parts and transient signal countermeasure parts should be installed at each electrical intrusion point. Moreover, the potential of an effective anti-drone system construction method for protecting important national facilities from drones used for malicious intent, such as criminal activities or terrorism, via the establishment of HPM sources based on the MILO system and analysis of the intentional EMP environment is high. As shown in Fig. 18, it is effective to secure flexibility to ensure that the means to disable cruise missiles, UAVs, and drones can be selectively used based on the operational environment by inducing the soft kill method and hard kill method. This implies that

an illegal drone pre-management system that involves mixing and overlapping operation of detection assets, determining appropriate countermeasures, and building neutralization measures should be established. Hence, building a protection system for important national facilities via the operation of this type of comprehensive and complex anti-drone system is urgently required. This can be elucidated by the contradiction between a spear and shield. Hence, when anti-drone technology is developed, drone technology also evolves to avoid anti-drone systems. As the sharpness of a drone's window increases, the robustness of an anti-drone defense system should correspondingly increase. It is difficult to find a system that can solve all of these constraints. Hence, it is possible to create a safe environment only when a complex and convergent protection system, which utilizes the strengths of each technology, is built and if the defense network can be strongly duplicated.

VI. CONCLUSION

In this paper, a high-power electromagnetic wave generating oscillator termed as MILO, which is typically used in the HPM field, was used. The performance of the MILO system was verified via several experimental studies for more than 15 years. The specifications of this system correspond to an output of up of 3 GW at an operating frequency of 1.15 GHz. Based on the MILO system, it was possible to create an intentional EMP environment, which can analyze effectiveness through the radiated electromagnetic wave electric field and power density value, for an effective distance and area to target an electronic device. Additionally, EMP protection technology is very important. Even if military standards are applied and if it exhibits the same performance specifications as those of the MILO system, then it can reduce the effects of temporary malfunction and damage within an effective distance of several kilometers to electronic devices equipped with protection facilities. Finally, it is expected that the results of this study will significantly contribute to the research on anti-drone technology for preventing security threats related to drone shooting of major military facilities and illegal information collection.

ACKNOWLEDGMENT

The authors would like to thank Editage (www.editage.co.kr) for English language editing.

REFERENCES

[1] S. H. Gold and G. S. Nusinovich, "Review of high-power microwave source research," *Rev. Sci. Instrum.*, vol. 68, no. 11, pp. 3945–3974, 1997.
[2] J. Benford, J. A. Swegle, E. Schamiloglu, *High Power Microwaes*, 3rd ed. Boca Raton, FL, USA: CRC Press, 2016.
[3] V. Kesari, B. N. Basu, *High Power Microwave Tubes: Basics and Trends*. San Rafael, CA, USA: Morgan & Claypool, 2018.
[4] H. L. Olesen, *Radiation Effects on Electronic Systems*, 1st ed. New York, NY, USA: Springer, 1966.
[5] F. Sabath, D. V. Giri, F. Rachidi, and A. Kaelin, *Ultra-Wideband, Short Pulse Electromagnetics*. New York, NY, USA: Springer, 2010.
[6] J. H. Booske, "Plasma physics and related challenges of millimeter-wave-to-terahertz and high power microwave generation," *Phys. Plasmas*, vol. 15, no. 5, May 2008, Art. no. 055502.
[7] K. S. H. Lee, *EMP Interaction Priniciples, Techniques, and Reference Data*. Santa Fe, NM, USA: Springer, 1986.
[8] S. Ibeobi and X. Pan, "Study of electromagnetic pulse (EMP) effect on surveillance unmanned aerial vehicles (UAVs)," *J. Mech. Eng., Autom. Control Syst.*, May 2021, doi: 10.21595/jmeacs.2021.21926.
[9] R. K. Parker, R. H. Abrams, B. G. Danly, and B. Levush, "Vacuum electronics," *IEEE Trans. Microw. Theory Techn.*, vol. 50, no. 3, Mar. 2002.
[10] E. Schamiloglu, "High power microwave sources and applications," in *IEEE MTT-S Int. Microw. Symp. Dig.*, Oct. 2004, pp. 6–11.
[11] T. H. G. G. Weise, M. Jung, D. Langhans, and M. Gowin, "Overview of directed energy weapon developments," in *Proc. 12th Symp. Electromagn. Launch Technol.*, Mar. 2005, pp. 25–28.
[12] G. Ni, B. Gao, and J. Lu, "Research on high power microwave weapons," in *Proc. Asia–Pacific Microw. Conf.*, Dec. 2006, pp. 4–7.
[13] S.-H. Min, O. Kwon, M. Sattorov, H. Jung, I.-K. Baek, S. Kim, J.-Y. Jeong, J. Jang, D. Hong, R. Bhattacharya, R. K. Barik, A. Bera, S. Park, J. Ahn, S. H. Lee, Y. J. Yoon, and G.-S. Park, "Effects on electronics exposed to high-power microwaves on the basis of a relativistic backward-wave oscillator operating on the X-band," *J. Electromagn. Waves Appl.*, vol. 31, no. 17, pp. 1875–1901, Jul. 2017.
[14] S.-H. Min, H.-C. Jung, G.-S. Park, J. Ahn, S. Heun Lee, Y. Joong Yoon, J. Kim, J.-H. Choi, and J. So, "Mode conversion of high-power electromagnetic microwave using coaxial-beam rotating antenna in relativistic backward-wave oscillator," *IEEE Trans. Plasma Sci.*, vol. 38, no. 6, pp. 1391–1397, Jun. 2010.
[15] S.-H. Min, O. Kwon, M. Sattorov, S. Kim, D. Hong, C. Park, B. H. Hong, I. S. Jung, I. Cho, W. T. Hwang, R. K. Barik, A. Bera, and G.-S. Park, "Low-level RF control of a klystron for medical linear accelerator applications," *AIP Adv.*, vol. 9, no. 2, Feb. 2019, Art. no. 025012.
[16] N. Kumar, U. Singh, T. P. Singh, and A. K. Sinha, "A review on the applications of high power, high frequency microwave source: Gyrotron," *J. Fusion Energy*, vol. 30, no. 4, pp. 257–276, Aug. 2011.
[17] I.-K. Baek, M. Sattorov, R. Bhattacharya, S. Kim, D. Hong, S.-H. Min, and G.-S. Park, "Origin of sideband and spurious noises in microwave oven magnetron," *IEEE Trans. Electron Devices*, vol. 64, no. 8, pp. 3413–3420, Aug. 2017.
[18] A. S. Gilmour, *Klystrons, Traveling Wave Tubes, Magnetrons, Crossed-Field Amplifiers, and Gyrotrons*. Norwood, MA, USA: Artech House, 2011.
[19] T. Xun, Y. Zhao, H. Yang, T. Hu, Z. Zhang, X.-B. Cheng, J. Zhang, J. Zhang, and H.-H. Zhong, "Developments of pulsed electron beam sources for high-power microwave applications," *IEEE Access*, vol. 8, pp. 101351–101358, 2020.
[20] M. Sattorov, D. Hong, S. Kim, H. Kwon, H. Kwon, S. Min, and G. Park, "Highly efficient compact gigawatt-level microwave source using relativistic electrons: Radial relativistic magnetron," *Electron. Lett.*, vol. 56, no. 11, pp. 556–559, May 2020.
[21] S.-H. Min, O. Kwon, M. Sattorov, H. Jung, S.-H. Shin, I.-K. Baek, S. Kim, S. Park, and G.-S. Park, "Characteristics of a transient axial mode from the formation of anode plasma in a gigawatt-class L-band magnetically insulated transmission line oscillator," *Phys. Plasmas*, vol. 23, no. 6, Jun. 2016, Art. no. 063120.
[22] Y. W. Fan, X. Y. Wang, Z. C. Zhang, T. Xun, and H. W. Yang, "A high-efficiency repetitively pulsed magnetically insulated transmission line oscillator," *Vacuum*, vol. 128, pp. 39–44, Jun. 2016.
[23] V. Nallasamy, S. K. Datta, S. U. Reddy, and P. K. Jain, "Advances and present trends in magnetically insulated line oscillator," *J. Electromagn. Waves Appl.*, vol. 31, no. 17, pp. 1864–1874, Jul. 2017.
[24] A. Kumar, P. Tripathi, S. Dwivedi, and P. K. Jain, "Analysis design and simulation of an axially partitioned dielectric loaded bi frequency MILO," *Defence Sci. J.*, vol. 71, no. 3, pp. 309–314, May 2021.
[25] J. Zhang, D. Zhang, Y. Fan, J. He, X. Ge, X. Zhang, J. Ju, and T. Xun, "Progress in narrowband high-power microwave sources," *Phys. Plasmas*, vol. 27, no. 1, Jan. 2020, Art. no. 010501.
[26] C. Wilson, *High Altitude Electromagnetic Pulse (HEMP) and High Power Microwave (HPM) Devices: Threat Assessments, CRS Report for Congress*, document RL32544, Jul. 2008.
[27] N. Eriksson, "Conceptual study of a future drone detection system," M.S. thesis, Dept. Ind. Mater. Sci., Chalmers Univ. Technol., Gothenburg, Sweden, 2018.
[28] M. G. Backstrom and K. G. Lovstrand, "Susceptibility of electronic systems to high-power microwaves: Summary of test experience," *IEEE Trans. Electromagn. Compat.*, vol. 46, no. 3, pp. 396–403, Aug. 2004.

[29] R. J. Capozzella, *High Power Microwaves on the Future Battlefield: Implications for U. S. Defense, a Research Report Submitted to the Faculty in Partial Fulfillment of the Graduation Requirements*. Arlington, VA, USA: U.S. Government, Feb. 2010.
[30] M. A. Holloway, *Overview of HPM Effects in Electronics, Short-Course at IPMHVC*, document LA-UR-12-21858, 2012.
[31] L. Palisek and L. Suchy, "High power microwave effects on computer networks—Sensitive parts and comparisons," *Int. J. Electromagn. Appl.*, vol. 2, no. 4, pp. 61–64, Aug. 2012.
[32] Z. Kelong, L. Shanwei, and Z. Yan, "Research on damage of intense electromagnetic pulse to radar receiving system," in *Proc. 5th Global Symp. Millim.-Waves*, May 2012, pp. 27–30.
[33] V. Gurevich, "Susceptibility of electronic components and equipment to HEMP: The facts and consequences," *Int. J. Res. Stud. Electr. Electron. Eng.*, vol. 4, no. 2, pp. 1–9, Feb. 2018.
[34] D. V. Giri, R. Hoad, F. Sabath, *High-Power Electromagnetic Effects on Electronic Systems*. Norwood, MA, USA: Artech House, 2020.
[35] I. N. Mindel, *DNA EMP Awareness Course Notes*, document Topical Report DNA 2772T, Oct. 1977.
[36] P. E. Nielsen, *Effects of Directed Energy Weapons*. Scotts Valley, CA, USA: Create Space Independent Publishing Platform, 2012.
[37] C. D. Taylor and D. V. Giri, *High-Power Microwave Systems and Effects*. New York, NY, USA: Taylor & Francis, 1994.
[38] S.-H. Min, H. Jung, O. Kwon, M. Sattorov, S. Kim, D. Hong, S. Kim, C. Park, I. Cho, M. Kim, K. M. Kim, W. T. Hwang, S. Park, K. C. Lee, Y. J. Lee, S. M. Lim, B. H. Hong, and G.-S. Park, "Performance of an impedance-variable pulsed high-power electron-beam accelerator based on energy efficient transmission," *Rev. Sci. Instrum.*, vol. 91, no. 11, Nov. 2020, Art. no. 113306.
[39] R. A. Poisel, *Information Warfare and Electronic Warfare Systems*. Norwood, MA, USA: Artech House, 2013.
[40] B. Zohuri, *Directed Energy Weapons—Physics of High Energy Lasers (HEL)*. Cham, Switzerland: Springer, 2016.
[41] B. Zohuri, *Directed-Energy Beam Weapons*. Cham, Switzerland: Springer, 2019.
[42] X. Jinshi, L. Wenhua, Z. Shiying, Z. Jinhua, and X. Changfeng, "Study of damage mechanism of high power microwave on electronic equipments," in *Proc. China-Japan Joint Microw. Conf.*, Sep. 2008, pp. 10–12.
[43] M. Ianoz, "A comparison between HEMP and HPEM parameters. Effects and mitigation methods," in *Proc. Asia–Pacific Symp. Electromagn. Compat. 19th Int. Zurich Symp. Electromagn. Compat.*, May 2008, pp. 275–278.
[44] *Requirements for the Control of Electromagnetic Interference Characteristics of Subsystems and Equipment*, document MIL-STD-461F, Dec. 2007.
[45] *Requirements for the Control of Electromagnetic Interference Characteristics of Subsystems and Equipment*, document CISPR 24, MIL-STD-461F, Dec. 2007.
[46] *High-Altitude Electromagnetic Pulse (HEMP) Protection for Ground-Based C41 Facilities Performing Critical, Time-Urgent Missions Part 1 Fixed Facilities*, document MIL-STD-188-125-1, Jul. 1998.
[47] *High-Altitude Electromagnetic Pulse (HEMP) Protection for Ground-Based C41 Facilities Performing Critical, Time-Urgent Missions Part 1 Transportable Systems*, document MIL-STD-188-125-2, Mar. 1999.
[48] *Electromagnetic Environmental Effects Requirements for Systems*, document MIL-STD-464C, Oct. 2010.
[49] D. V. Giri, W. D. Prather, and C. E. Baum, "The relationship between NEMP standards and simulator performance specifications," in *Sensor and Simulation Note 538*. Fort Belvoir, VA, USA: Defense Threat Reduction Agency, 2009.
[50] Y. Li, C. Chai, Y. Liu, Y. Li, H. Wu, W. Zhang, F. Li, and Y. Yang, "Upset and damage mechanisms of the three-dimensional silicon device induced by high power microwave interference," *IEICE Electron. Exp.*, vol. 16, no. 19, pp. 1–6, 2019.

SUN-HONG MIN was born in Chamsil, Seoul, South Korea, in February 1978. He received the B.S., M.S., and Ph.D. degrees in physics from the Department of Physics and Astronomy, Seoul National University (SNU), Seoul, in 2003, 2006, and 2013, respectively. He has studied high-power microwaves (HPM), mm-waves and THz vacuum electronics device (VED), THz-imaging technology, electrical electronics, pulse power machine, radiation physics, medical beam accelerator physics, and biophysics for calcium binding protein under paramagnetic resonance and non-thermal irreversible electroporation (NTIRE) over the past 17 years. His main fields for VEDs are BWO, MILO, klystron, magnetron, TWT, cyclotron, and synchrotron. He used to work as a Postdoctoral Researcher with the Center for THz-Bio Application System, Seoul National University, and a Senior Researcher with Seoul-Teracom Inc., Seoul, from 2013 to 2015. He worked as a Senior Researcher with the Department of the Division of Heavy-ion Clinical Researches, Korea Heavy Ion Medical Accelerator Project (KHIMA), Korea Institute of Radiological and Medical Science (KIRAMS). He currently works as a Senior Researcher with the Department of RI Application, Medical Accelerator Research Team, Korea Institute of Radiological and Medical Sciences (KIRAMS). He is also performing several projects on boron neutron capture therapy (BNCT) and bio-terahertz (THz) convergence, as a Senior Research Associate, Concurrent position at the Center for THz-Driven Biological Systems, Department of Physics and Astronomy, Advanced Institute of Convergence Technology (AICT), Seoul National University. In addition, he is working as an Advisory Member and proposal evaluation committee for the future challenge defense technology development project hosted by the Defense Acquisition Program Administration and the Agency for Defense Development.

HOECHUN JUNG was born in Gwangju, South Korea, in August 1976. He received the B.S. degree in physics education from Seoul National University (SNU), Seoul, South Korea, in 2001, and the Ph.D. degree from the Department of Physics and Astronomy, SNU, in August 2009. He studied on gigawatt-level backward-wave oscillator and a magnetically insulated line oscillator as a kind of HPEM source. He worked with LIG Nex1 Company Ltd., Gyeonggi-do, South Korea, from 2009 to 2012. He has been working as a Senior Researcher with the Rare Isotope Science Project, Institute for Basic Science, Daejeon, South Korea, since 2012.

OHJOON KWON received the B.S., M.S., and Ph.D. degrees in physics from Seoul National University, Seoul, South Korea, in 2002, 2008, and 2016, respectively. He has involved in terahertz vacuum electron devices and their biological effects. He is currently working as a Senior Researcher with the Institute for Basic Science, Center (IBS) for Axion and Precision Physics Research, Daejeon, South Korea.

MATLABJON SATTOROV received the B.S. and M.S. degrees (Hons.) in physics from Samarkand State University, Samarkand, Uzbekistan, in 1998 and 2000, respectively, and the Ph.D. degree in physics from Seoul National University, Seoul, South Korea, in 2012. From 1998 to 2000, he was a High School Teacher. From 2000 to 2005, he was the Head of the Center for Technical Support of International Affairs and a Teaching Assistant with the Department of Physics, Samarkand State University. He won the Graduate Scholarship for excellent foreign students grant and joined the Department of Physics and Astronomy, Seoul National University. He is currently a Research and Development Director of Seoul-Teracom Inc., Seoul, and a Senior Scientist with Seoul National University. He has authored or coauthored more than 87 publications in peer-reviewed journals and conferences. He is working on terahertz vacuum electron devices, such as clinotron, orotron, backward wave oscillator, and extended interaction oscillator.

SEONTAE KIM received the B.S. degree in physics from Hankuk University of Foreign Studies, Seoul, South Korea, in 2009, and the Ph.D. degree from the Department of Physics and Astronomy, Seoul National University, Seoul, in 2018. He currently works as a Postdoctoral Researcher position with the Center for THz-Driven Biological Systems, Department of Physics and Astronomy, Seoul National University. He is also working at Young IN ACE, Dongan-gu, Anyang-si, Gyeonggi-do, South Korea.

SEUNG-HYUK PARK was born in Uijeongbu, South Korea, in 1980. He received the B.S. degree in physics from Kookmin University, Seoul, South Korea, in 2004, and the M.S. degree in physics and astronomy from Seoul National University, Seoul, in 2011. He joined Hanwha Corporation, Seoul, where he is currently a Senior Researcher Engineer. His current research interests include applied computational electromagnetics and high power microwave.

DONGPYO HONG received the B.S. degree in physics from Sogang University, Seoul, South Korea, in 2014, and the Ph.D. degree in physics from the Department of Physics and Astronomy, Seoul National University, Seoul, in 2021. He received his Ph.D. with the title "Experimental Study on Highly Electrically Conductive Reduced Graphene Oxide Free-standing Film." He has been a Postdoctoral Researcher with the Center for THz-Driven Biomedical Systems, Seoul National University, and the Institute of Applied Physics, Seoul National University, since 2021. His specialties include physics based on beam-dynamics, as well as high-power microwave engineering, RF engineering, and applied physics based on millimeter wave and terahertz wave physics.

SEONMYEONG KIM was born in Seoul, South Korea, in 1991. He received the B.S. and Ph.D. degrees in physics from the Department of Physics and Astronomy, Seoul National University, Seoul, in 2014 and 2021, respectively. He studied hydrogen-bond structure and low-frequency dynamics of water in electrolyte solution and lipid bilayer system by the method of dielectric relaxation spectroscopy, classical MD simulation and ab-initio MD simulation. His main field is understanding water and hydrogen bond network's key role in biochemical sciences, such as ultrafast energy transfers and relaxation through hydrogen bonding network of water. He has been a Postdoctoral Researcher at the Center for THz-Driven Biomedical Systems, Seoul National University, and the Institute of Applied Physics, Seoul National University, since 2021.

CHAWON PARK received the Ph.D. degree in physics from Korea University, Seoul, South Korea, in 2004.

From April 2004 to February 2006, he was a Postdoctoral Researcher with the Department of Physics, Sungkyunkwan University. From August 2006 to July 2007, he was a Researcher with the School of Physics and Astronomy, Seoul National University. From August 2007 to January 2010, he was a Professor with the Department of Physics, Sungkyunkwan University. From January 2010 to February 2013, he was a Research Professor with the Department of Physics, University of Seoul. Since March 2013, he has been a Senior Researcher with the Department of RI Application, Medical Accelerator Research Team, Korea Institute of Radiological and Medical Sciences (KIRAMS). His main research interests include accelerator beam physics and beam diagnosis, high energy particle physics, medical accelerator design, applied physics using low energy particle beams, and license for radiation generator (RG) facilities.

BONG HWAN HONG received the Ph.D. degree from the Department of Mechanical Engineering from Yonsei University, Seoul, South Korea, in 2012. He currently works as the Principal Researcher with the Team Leader at the Department of RI Application, Medical Accelerator Research Team, Korea Institute of Radiological and Medical Sciences (KIRAMS). He is also performing as the Principle Investigator (PI) of the projects on boron neutron capture therapy (BNCT) at KIRAMS.

ILSUNG CHO received the Ph.D. degree in physics from Sungkyunkwan University, Seoul, South Korea, in 2006.

From June 2006 to June 2009, he was a Postdoctoral Researcher with the BK21 Physics and Applied Physics Research Group, Yonsei University. From September 2009 to February 2011, he was a Senior Researcher with the Medical Industry Research Institute, Kyung Hee University. From March 2011 to April 2014, he was a Medical Physics Resident with Asan Medical Center, Seoul. Since January 2014, he has been a Senior Researcher with the Department of RI Application, Medical Accelerator Research Team, Korea Institute of Radiological and Medical Sciences (KIRAMS). His main research interests include high energy particle physics, radiation therapy physics, radiation therapy, radiation surgery, medical device international standard (IEC TC62/SC C), and national standard, Ministry of Food and Drug Safety.

SUKHWAL MA received the Ph.D. degree in plasma physics from Jeonbuk National University, Jeonju, South Korea, in 2019. From August 2011 to June 2019, he was a Researcher with the Institute of Plasma Technology, Korea Institute of Fusion Energy, Gunsan, South Korea. From July 2019 to August 2020, he was a Postdoctoral Researcher with the Radwaste Management Center, Korea Atomic Energy Research Institute, Daejeon, South Korea. Since September 2020, he has been a Senior Researcher with the Department of RI Application, Medical Accelerator Research Team, Korea Institute of Radiological and Medical Sciences (KIRAMS). His main research interests include atmospheric pressure plasma application, including environment, bio-medical, and energy and material processing. He is currently interested in research on medical accelerators and is working on the structural design of gas stripper and accelerator system regarding boron neutron capture therapy (BNCT) at KIRAMS.

MINHO KIM received the B.S. degree in radiologic science from Korea University, Seoul, South Korea, in 2012, and the M.S. and Ph.D. degrees from the Department of Bio-Convergence Engineering from Korea University, in 2014 and 2019, respectively. He is currently working as a Senior Researcher with the Department of RI Application, Medical Accelerator Research Team, Korea Institute of Radiological and Medical Sciences (KIRAMS). His main research interests include radiation detection, radiation imaging, Monte-Carlo simulation, and BNCT.

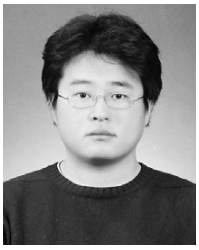

YOUNG JOON YOO received the B.S., M.S., and Ph.D. degrees in physics from the Department of Physics, Hanyang University, Seoul, in 2003, 2005, and 2014, respectively. He received the Ph.D. with the title ''Studies on perfect-absorption properties and multiple magnetic resonances of metamaterials.'' He has been a Senior Researcher with the Center for Applied Electromagnetic Research, Advanced Institute of Convergence Technology, since 2019. His specialties include physics based on electromagnetic metamaterials, as well as long range transmitter, absorber, and applied physics based on millimeter wave for 5G and 6G systems.

SANG YOON PARK is currently the President of the Advanced Institute of Convergence Technology, Center for Applied Electromagnetic Research. This centre was established with the goal of conducting leading research in the space-time wave control field based on organic/inorganic nanomaterials and establishing applied technologies in the energy, environment, and bio fields. They are conducting research to secure the original technology of wave control and nanomaterials and apply them to application technologies, such as wearable devices, bio-signal detection, and energy storage.

GUN-SIK PARK (Senior Member, IEEE) received the B.S. degree in physics education from Seoul National University, Seoul, South Korea, in 1978, and the Ph.D. degree in physics from the University of Maryland, College Park, MD, USA, in 1989. In 1987, he was with the Naval Research Laboratory, Washington, DC, USA, through Omega-P Inc. Since 1995, he has been with Seoul National University, where he is currently a Professor with the Department of Physics and Astronomy and also jointly with the Department of Electrical Engineering. From 2000 to 2008, he was the Director for the National Research Laboratory for Vacuum Electro-physics and High-Power Terahertz Radiation supported by the Ministry of Education, Science, and Technology of Korea. Since 2009, he has been the Director for the Center for THz-Bio Application Systems, Seoul National University, supported by the Ministry of Education, Science, and Technology of Korea. He is currently the CEO of Seoul-Teracom Inc., Seoul. He is also the Head of research at the Center for THz-Driven Biological Systems, Department of Physics and Astronomy, Seoul National University. He has authored over 100 peer-reviewed journal publications from the areas of high-power microwaves to terahertz waves. He has been a Technical Committee Member of the IEEE Electron Devices Society in Vacuum Electronics, since 1999, and a Board Member for the International Society of Infrared, Millimeter, and Terahertz Waves, since 2010. He serves as an organizing committee member, an advisory committee member, and a program committee member for a number of international conferences. He was a 2021 recipient of John R. Pierce for excellence in vacuum electronics of IEEE EDS. He has founded the International THz-Bio Workshop, from 2010 to 2016. He served as the Conference Chair for the Fourth IEEE International Vacuum Electronics Conference, in 2003, and the Conference Co-Chair for the 34th International Conference on Infrared, Millimeter, and Terahertz Waves, in 2009. He was the Chairman of the International Society of Infrared, Millimeter and Terahertz Waves (IRMMW-THz), from 2015 to 2018. He serves as the Vice Chairman for Korea Terahertz Forum. He has been an Editorial Board Member for the journal of *Terahertz Science and Technology* and a Topic Editor for the IEEE TRANSACTIONS ON TERAHERTZ SCIENCE AND TECHNOLOGY, since 2011.